linium ion to one bromine. This would, however, be necessary to form three hydrogen bonds to the Br^- ion.

Hydrogen Bonds in Amino Acid Hydroiodides

Considering the hydroiodides (Table 4) we have not to rely on the ^{127}I frequencies, but the nuclear quadrupole interaction energy $e^2\phi_{zz}Qh^{-1}(^{127}I)$ and the asymmetry parameter η of the interaction tensor are available. Three compounds have been studied here. Two of them, $(Gly)_2 \cdot NaI \cdot H_2O$ and Sem · HI, show at room temperature $e^2\phi_{zz}Qh^{-1}(^{127}I)$ between 116 and 119 MHz, η being between 0.70 and 0.96, whereas for Leu · HI the nuclear quadrupole coupling constant of ^{127}I is 156 MHz, $\eta = 0.66$. It is interesting to note that a slight sigmoidal character of $e^2\phi_{zz}Qh^{-1}(^{127}I)$ and of $\eta(^{127}I)$ is observed in the temperature dependence of these two parameters for Leu · HI, the hydrobromide of which shows a phase transition at 331.6 K.

In spite of small experimental evidence we conclude, that as in case of ^{79}Br – NQR frequencies of amino acid hydrobromides also by $e^2\phi_{zz}Qh^{-1}(^{127}I)$ of the amino acid hydroiodides a weaker and a stronger hydrogen bond system Y – H...halogen can be distinguished. This conclusion is supported by the crystal structure information available for $(Gly)_2 \cdot NaI \cdot H_2O$. This compound crystallizes with the space group $P2_1/c$, $Z = 4$ [25] and the iodine ion is involved in three $N^+ - H...I^-$ hydrogen bonds. In crystalline Sem · HI such $N^+ - H...I^-$ hydrogen bonds are possible only. On the other hand Leu · HI [21] is isostructural with Leu · HBr (space group $P2_12_12_1$, $Z = 4$) and has the solid state bond configuration:

$$1 \times O-H...I^-, \quad 2 \times N^+-H...I^-, \quad 1 \times N^+-H...O^=,$$

proving the proposed correlation between the hydrogen bonding scheme of a halide ion and its NQR-frequency.

We are grateful to the Deutsche Forschungsgemeinschaft and to the Fonds der Chemischen Industrie for support of this work. We are also grateful to Mr. Da Zhang for help in some measurements.

References

[1] W. Pies and Al. Weiss, Bull. Chem. Soc. Jpn. *51*, 1051 (1978).
[2] W. Pies, M. Shahbazi, and Al. Weiss, Ber. Bunsenges. Phys. Chem. *82*, 594 (1978).
[3] G. Fecher, Al. Weiss, W. Joswig, and H. Fuess, Z. Naturforsch. *369*, 956 (1981).
[4] G. Fecher, Al. Weiss, and G. Heger, Z. Naturforsch. *36a*, 967 (1981).
[5] V. G. Krishnan and Al. Weiss, Ber. Bunsenges. Phys. Chem. *87*, 254 (1983).
[6] V. G. Krishnan and Al. Weiss, J. Mol. Struct. *111*, 379 (1983).
[7] Seshu Bai and Al. Weiss, Z. Naturforsch. *39a*, 366 (1984).
[8] G. Fecher and Al. Weiss, to be published.
[9] G. Jugie and J. A. S. Smith, J. Chem. Soc., Faraday Trans. II, *74*, 994 (1978).
[10] H. Budak, M. L. S. Garcia, I. C. Ewart, I. J. F. Poplett, and J. A. S. Smith, J. Magn. Reson. *35*, 309 (1979).
[11] W. Pies and Al. Weiss, J. Magn. Reson. *30*, 469 (1978).
[12] D. Bougard, Ber. Bunsenges. Phys. Chem. *87*, 279 (1983).
[13] J. Frausto da Silva and L. Vilas Boas, Rev. Port. Quim. *14*, 115 (1972).
[14] T. Hahn, Z. Kristallogr. *111*, 161 (1959).
[15] E. Lippincott and R. Khanna, Colloq. Spectrosc. Int., 12th, Exeter, 513, England 1965.
[16] G. Pimentel and A. McClellan, Ann. Rev. Phys. Chem. *22*, 347 (1971).
[17] E. Subramanian, Acta Crystallogr. *22*, 910 (1967).
[18] A. R. Al-Karaghouli, F. E. Cole, M. S. Lehmann, C. F. Miskell, J. J. Verbist, and T. F. Koetzle, J. Chem. Phys. *63*, 1360 (1975).
[19] T. F. Koetzle, L. Golic, M. S. Lehmann, J. J. Verbist, and W. C. Hamilton, J. Chem. Phys. *60*, 4690 (1974).
[20] R. Parthasarathy and R. Chandrasekaran, Ind. J. Pure Appl. Phys. *4*, 293 (1966).
[21] M. Chaney, O. Seely, and K. Steinrauf, Acta Crystallogr. *B27*, 544 (1971).
[22] T. Hahn and M. J. Buerger, Z. Kristallogr. *108*, 419 (1957).
[23] P. Piret, J. Meunier-Piret, J. Verbist, and M. van Meerssche, Bull. Soc. Chim. Belg. *81*, 539 (1972).
[24] L. Golic and W. C. Hamilton, Acta Crystallogr. *B28*, 1265 (1972).
[25] J. Verbist, J. Putzeys, P. Piret, and M. van Meerssche, Acta Crystallogr. *B27*, 1190 (1971).

(Eingegangen am 14. Mai 1984) E 5723

Electron Transfer Reactions at n-GaP (100) and (111) in Acetonitrile Solutions Facilitated by Cation Adsorption

R. McIntyre and H. Gerischer

Fritz-Haber-Institut der Max-Planck-Gesellschaft, Faradayweg 4–6, D-1000 Berlin 33, West Germany

Adsorption / Aprotic Electrolytes / Photoelectrochemistry / Semiconductors

Electron transfer reactions occurring at n-GaP (111) and (100) electrodes have been investigated in acetonitrile solutions. In the presence of strongly oxidising cations, such as 10-methylphenothiazine ($10\text{-}MP^{+\cdot}$), Ferrocene (Cp_2Fe^+) and tetrathiafulvalen ($TTF^{+\cdot}$), it is shown that electron transfer proceeds directly from the conduction band to cations adsorbed at the semiconductor surface. Differential capacitance and photo/dark-current measurements have been used to identify a considerable positive shift of the flatband potential (U_{FB}) in the presence of the oxidising cation. This phenomenon is absent in the presence of a similarly oxidising neutral species. No evidence was obtained to support the model which proposes mediated electron transfer via surface states deep in the band gap.

Introduction

Kohl and Bard [1] have recently reported the electroreduction of cations at several semiconductor electrodes, in the absence of illumination, at potentials observed to be well positive of U_{FB}. This phenomenon cannot be rationalized on the basis of the classical theory [2] and therefore they propose a model which predicts that within the band gap region intermediate traps or surface states exist which can mediate electron transfer between

the semiconductor and solution [1]. Thus the reduction of solution species can occur, isoenergetically, at potentials apparently well positive of U_{FB}, near the surface level energy of the proposed trap. For example, the reduction of 10-$MP^{+\cdot}$ at n-GaP (111) is reported to occur at a potential ~ 1.7 V positive of U_{FB}. To explain this behaviour the existence of a low-lying trap was postulated, the potential-dependent rate at which electrons fill the trap being necessarily greater at the reduction potential than the rate of diffusion of the electroactive species. When the Fermi level of the semiconductor becomes lower than the trap level the process is effectively switched-off.

There are three obvious circumstances which can cause electron transfer to occur at potentials "apparently" well positive of U_{FB} for a highly oxidising redox couple. First, the situation where a high density of intrinsic surface states empty into the oxidised component of the redox couple leaving behind a positive surface charge and consequently a positive shift in U_{FB} occurs. Second, the situation where the positive species adsorb and thereby cause a positive shift in U_{FB}. Third, under reverse bias conditions, hole injection into the valence band can also result in the aforementioned positive shift in U_{FB}, however this situation is relatively easy to identify, see later. Unfortunately, for cases 1 and 2 the final state for both situations can, effectively, be the same and therefore it is very difficult to distinguish between the two. In principle, however, a very clear distinction does exist. In the first case the extent to which U_{FB} moves depends on the redox potential of the particular redox couple. The degree to which band bending occurs for surface states localized at a particular energy should always be controlled by the difference between the energy of the surface state and the respective band edge energy. This is shown in Fig. 1 A for an n-type material in contact with two different redox systems. In the second case the extent to which U_{FB} moves depends on the degree to which adsorption occurs, band bending however should be controlled by both adsorption and the redox potential of the couple. This is shown in Fig. 1 B for n-type material in contact with three different redox couples, with equivalent redox potentials, which exhibit different properties with respect to adsorption. This distinction is of considerable importance with respect to photoelectrochemical energy conversion. Whilst both cases will manifest themselves as a decrease in the obtainable photovoltage, due to a smaller band bending in the dark, the former case should be independent of whether the oxidised species is positively charged or neutral, whereas the latter will be strongly dependent on this criterion.

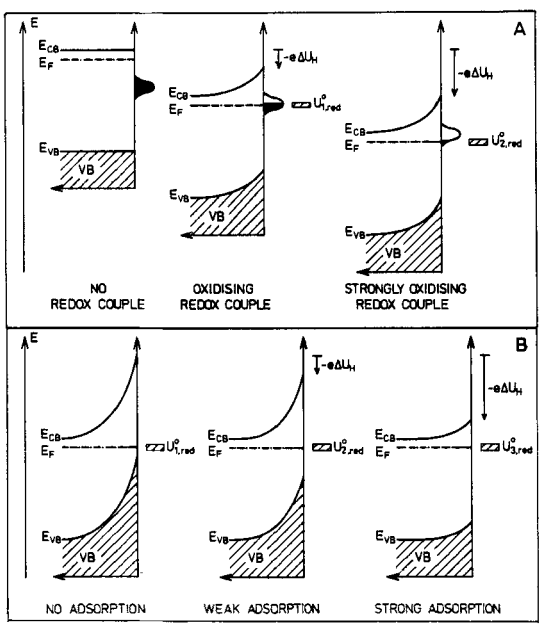

Fig. 1
Schematic representation of the potential distribution for a semiconductor/electrolyte interface in the presence of strongly oxidising redox couples for situation A – a large concentration of surface states, B – cation adsorption

In this communication we will present evidence to support a model which proposes that the adsorption of highly oxidising cations at n-GaP electrodes causes a considerable positive shift in the positions of the band edges which facilitates electron transfer in the cathodic direction.

2. Experimental

Single crystal n-GaP (111) and (100) wafers, doped with sulphur ($N_D = 2 \cdot 10^{17}$ cm^{-3}) and tellurium ($N_D = 1 \cdot 10^{18}$ cm^{-3}) respectively, were obtained from Cambridge Instruments. Ohmic contacts were achieved by vapour phase In deposition, followed by annealing at 600°C for 20 min under a hydrogen atmosphere. The electrode pretreatment involved etching with Br_2/MeOH solution, cleaning with conc. HCl followed by washing with water and finally acetonitrile (ACN). ACN was purified by fractional distillation, using a modified Widmer column, following a procedure described elsewhere [3]. 10-Methylphenothiazine (10-MP) was prepared from phenothiazine (Merck) by refluxing with Me_2SO_4 in the presence of KOH, K_2CO_3 and 5M% Aliquot 336 phase transfer catalyser. The final product was recrystallised, twice from EtOH and once from ACN, and dried under vacuum for 24 h at 110°C, final Mpt = 101.5°C Tetrachloro-o-benzoquinone was prepared by a method described elsewhere [4], recrystallised three times from ether and dried under vacuum, final Mpt = 127°C. Tetrathiafulvalen (Fluka) was recrystallised twice from hexane washed with ethanol and dried under vacuum, final Mpt = 120.5°C [5]. Ferrocene (Fluka) was recrystallised three times from 50% H_2O/EtOH and dried under vacuum at 50°C, final Mpt = 172.5°C [6]. The support electrolyte tetramethylammonium tetrafluoroborate (TMABF) (Fluka) was recrystallised five times from H_2O and dried under vacuum for 24 h at 120°C.

The photocurrent measurements were made by illuminating the electrodes with a tungsten halogen light source 12 V/100 W, the light source intensity was controlled using Schott NG-4 neutral density filters 0.5 and 0.2. A Bausch & Lomb monochromator with infrared grating was used to obtain monochromatic light with a wavelength range of 500 nm – 1100 nm. The electrochemical cell was a conventional, three compartment cell (approx volume 5 cm^3). The working compartment contained an auxiliary Pt wire electrode which was used as a pre-electrolysis electrode to produce the oxidising cations. The working and counter electrode ports were quick-fit joints with silicon-ring seals. Using this particular design the cell could be adequately sealed to function outside the dry box. The reference electrode was an Ag/Ag^+, 10^{-4} M ($AgNO_3$), 0.5 M TMABF. Contact to the working compartment was achieved as a result of ionic conduction through a Pt/glass (Duran) seal.

Differential capacitance measurements were recorded as a function of applied potential by scanning the potential at 10 mVs^{-1}. Using a lock-in amplifier (PAR model HR-8), with an internal oscillator, an ac signal with a 10 mV amplitude was used to modulate the applied potential. The capacitance values were extracted from the quadrature component of the output.

3. Results

3.1. 10-Methylphenothiazine (10-MP)

Flatband potentials were determined by regression analyses of Mott-Schottky data. The Mott-Schottky plots derived from differential capacitance measurements are shown in Fig. 2. A positive shift in the value

Table 1

Frequency Hz	n-GaP (100)				n-GaP (111)			
	10-MP		$10\text{-MP}^{+\cdot}$		10-MP		$10\text{-MP}^{+\cdot}$	
	$-U_{FB}$/V	$N_D \cdot 10^{-18}$/cm^{-3}	$-U_{FB}$/V	$N_D \cdot 10^{-18}$/cm^{-3}	$-U_{FB}$/V	$N_D \cdot 10^{-17}$/cm^{-3}	$-U_{FB}$/V	$N_D \cdot 10^{-17}$/cm^{-3}
100	2.39	2.87	1.28	2.58	1.84	1.34	1.16	1.29
300	2.21	2.40	1.19	2.33	1.76	1.21	1.03	1.09
1.000	2.20	2.38	1.13	2.41	1.78	1.15	1.01	1.05
4.800	2.28	2.75	1.07	2.27	–	–	–	–

of U_{FB} of approx. 1.0 V is observed which is dependent on the presence or absence of $10\text{-MP}^{+\cdot}$. A comprehensive set of data is shown in Table 1, within experimental error the results are relatively independent of frequency over the range 100 Hz to 4.8 kHz and independent of the concentration of $10\text{-MP}^{+\cdot}$ above 1 mM. The positive shift in U_{FB} could be reversibly produced, after exposure of the electrode to the $10\text{-MP}^{+\cdot}$ solution, by simply repeating the cleaning procedure outlined in section 2. The reproducibility of the capacitance measurements with duplicate trials at a given frequency was excellent in the region where the dark current was $\leq 0.8\ \mu A\ cm^{-2}$. In this region the hysteresis was negligible and independent of whether the results were recorded point by point, in random order, or with a sweep rate $\leq 10\ mVs^{-1}$. The values of the donor density extracted from the Mott-Schottky plots were shown to correspond well with those given by the manufacturer (see section 2 and Table 1 for comparison).

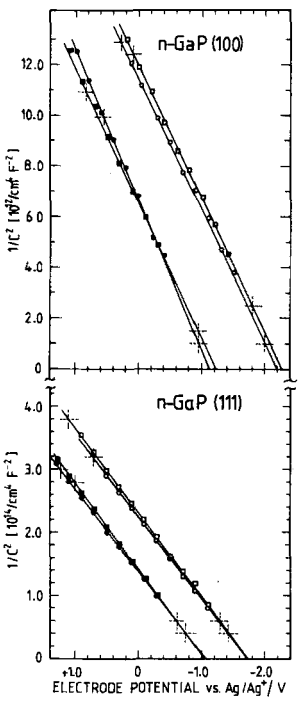

Fig. 2
Mott-Schottky plots for n-GaP (100) and n-GaP (111) in the absence of $10\text{-MP}^{+\cdot}$, ○ – 1 kHz, □ – 300 Hz and in the presence of $10\text{-MP}^{+\cdot}$ (~ 1 mM), ● – 1 kHz, ■ – 300 Hz

For ACN solutions containing TMABF the Pt electrode can be shown to be perfectly polarisable over a potential range of at least −2.5 to +2.0 V vs Ag/Ag^+. The oxidation of 10-MP at the Pt electrode in ACN/(0.5 M) TMABF is shown in Fig. 3. The 10-MP/$10\text{-MP}^{+\cdot}$ couple appears fully reversible with $U^0 \sim +0.4$ V, further oxidation to the 10-MP^{2+} species is shown to be an irreversible process occurring at $U^0 \sim +1.0$ V, cf. Ref. [7]. Current-potential curves obtained for n-GaP (100), in the above solution, are also shown. Curves 1 and 2 are photocurrent curves obtained with neutral density attenuating filters 0.5 and 0.2 respectively, the magnitude of the limiting current

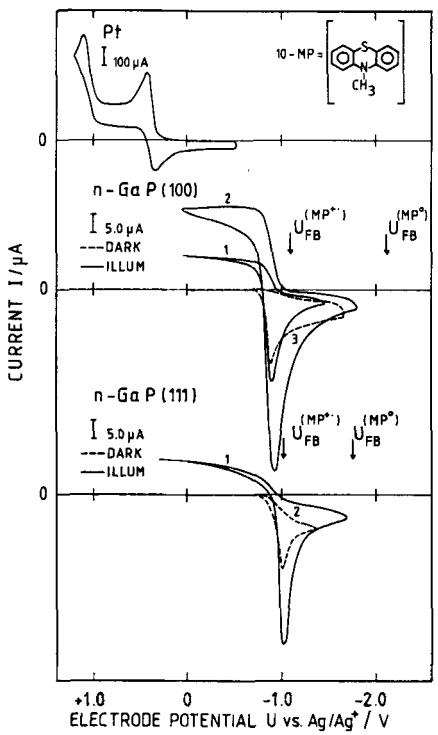

Fig. 3
Current-potential curves for ACN/TMABF (0.5 M), $10\text{-MP}^{+\cdot}$ (0.026 M), sweep rate 0.05 V s^{-1}: for Pt ($A \sim 1.0\ cm^2$); for n-GaP (100) ($A = 0.11\ cm^2$), 1. Illum. ×0.5 attenuation, 2. Illum. ×0.2 attenuation, 3. Dark current in the presence of $10\text{-MP}^{+\cdot}$ (~ 1.5 mM); for n-GaP (111) ($A = 0.09\ cm^2$), 1. Illum. ×0.2 attenuation, 2. Dark current in the presence of $10\text{-MP}^{+\cdot}$ (~ 1.2 mM)

value, observed at positive potentials, indicates that the rate determining step for the photoanodic process is the photogeneration of electron-hole pairs. Notice that the reduction process begins at a potential well positive of $U_{FB}^{(MP^0)}$, but close to $U_{FB}^{(MP^{+\cdot})}$. Curve 3 shows the dark current observed in the presence of $10\text{-MP}^{+\cdot}$ (≤ 1.0 mM); the reduction process is observed at the same potential as under illumination and the anodic process is absent. Now, compare the data obtained for n-GaP (100) with data obtained in the same solution for n-GaP (111), the results are shown to be qualitatively very similar. The quantitative differences arise from the different value of $U_{FB}^{(MP^0)}$. This behaviour can be explained in terms of a change in the surface dipole in going from a (100) surface to a (111) surface. Recently, UHV studies have shown that the electron affinity for the (111) GaAs surface can be up to 0.4 V lower than for the (100) surface [8]. This result was interpreted in terms of a (111) surface terminated with an essentially complete Ga-surface layer compared with a (100) surface terminated with a predominantly As-surface layer. Due to the ionicity of the GaAs bond the two surfaces exhibit a relatively positive and relatively negative surface dipole, respectively. Although in our case, after etching and cleaning, one can merely speculate as to the exact surface composition, the positive shift in the value of U_{FB} for n-GaP (111) could be explained in terms of a

relatively positive surface dipole for the (111) surface*). In the presence of 10-$MP^{+\cdot}$ the value of U_{FB} was again observed to be shifted by approx. 0.60 V to a more positive potential. Although the shift appears to be somewhat less for the (111) surface compared with the (100) surface, in both cases the value of U_{FB} coincides reasonably well with the onset of the current, due to the reduction of 10-$MP^{+\cdot}$.

Further evidence, which is quantitatively in agreement with the change in values of the band edge positions for n-GaP (111) and (100) in the presence of 10-$MP^{+\cdot}$, has recently been obtained from electroluminescence measurements. The predicted shift in the onset of luminescence with respect to potential, as a consequence of $\Delta U_{FB}^{(100)} = +1.0$ V and $\Delta U_{FB}^{(111)} = +0.6$ V, has been observed [10].

3.2. Ferrocene (Cp_2Fe)

The ferrocene cation Cp_2Fe^+ is also strongly oxidising and was chosen for comparison with 10-$MP^{+\cdot}$. Fig. 4 shows the comparison of the Mott-Schottky plots in the presence and absence of Cp_2Fe^+ (≤ 2 mM), once again a large positive shift is observed, $\Delta U_{FB}^{(100)} = +0.8$ V. The photo/dark-current measurements shown in Fig. 5 for the Cp_2Fe/Cp_2Fe^+ couple are qualitatively very similar to those observed for the 10-MP/10-$MP^{+\cdot}$ couple.

3.3. Tetrathiafulvalen (TTF)

The tetrathiafulvalen cation $TTF^{+\cdot}$ is another strongly oxidising cation which, unlike Cp_2Fe^+, has an exposed positive charge, similar to 10-$MP^{+\cdot}$, and should adsorb quite strongly with respect to Cp_2Fe^+. Fig. 6 shows a comparison of the Mott-Schottky plots in the presence and absence of $TTF^{+\cdot} \leq 0.06$ mM. $\Delta U_{FB}^{(100)}$ is observed to be ~ 1.0 V which is larger than that observed for Cp_2Fe^+ despite the lower concentration. The photo/dark-current measurements, Fig. 7, are once again shown to be qualitatively very similar to those obtained for 10-$MP^{+\cdot}$ and Cp_2Fe^+.

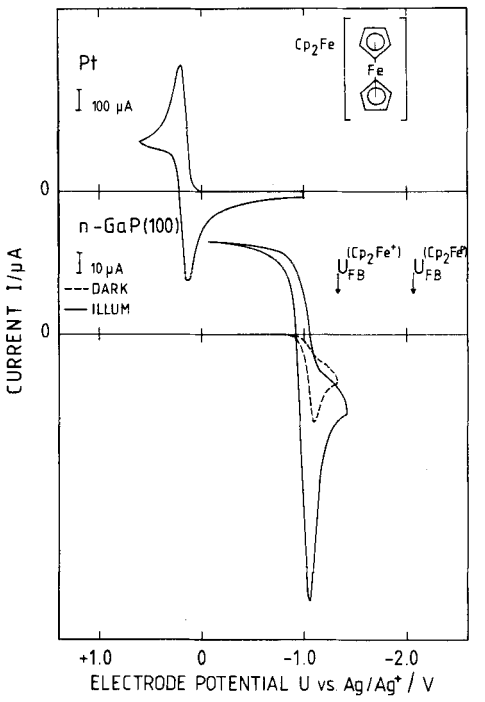

Fig. 5
Current-potential curves for ACN/TMABF (0.5 M), Cp_2Fe^+ (0.044 M), sweep rate 0.10 V s^{-1}: for Pt ($A \simeq 1.0$ cm^2); for n-GaP (100) ($A = 0.1$ cm^2), 1. Illum. ×0.5 attenuation, 2. Dark – in the presence of Cp_2Fe^+ (~ 2 mM)

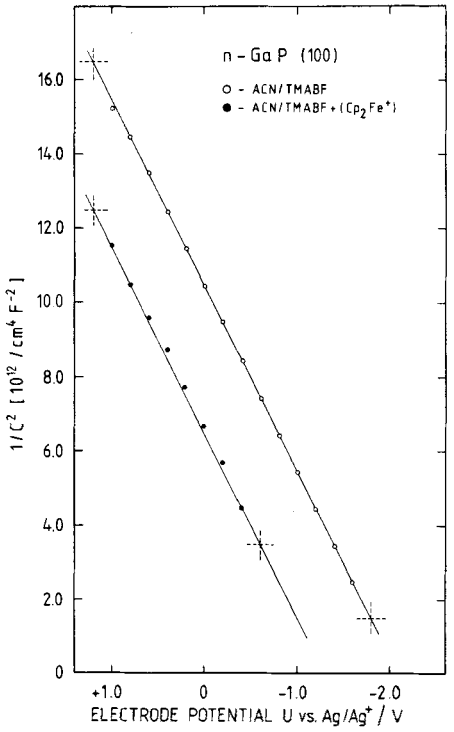

Fig. 4
Mott-Schottky plots for n-GaP (100) in the absence of Cp_2Fe^+, ○ – 1 kHz and in the presence of Cp_2Fe^+, ● – 1 kHz

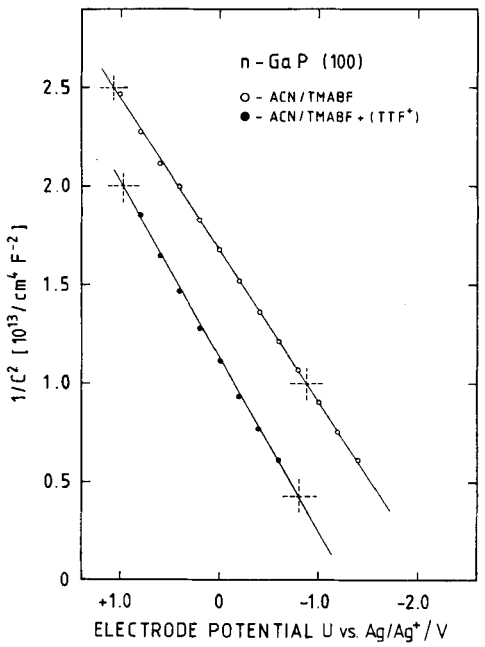

Fig. 6
Mott-Schottky plots for n-GaP (100) in the absence of $TTF^{+\cdot}$, ○ – 1 kHz, and in the presence of $TTF^{+\cdot}$, ● – 1 kHz

*) The Ga-truncated (111) surface, as opposed to the P-truncated ($\bar{1}\bar{1}\bar{1}$) surface, was confirmed by an etching procedure described by Meek & Schumaker [9]. The surface should remain predominantly Ga after the cleaning procedure described above [9].

3.4. Tetrachloro-o-benzoquinone (o-TCBQ)

As a result of the negative inductive effect of the chloride functionalities, o-TCBQ is a highly electrophilic neutral species which is almost as strongly oxidising as the $TTF^{+\cdot}$ cation, see Fig. 9. Therefore a comparison of the photoelectrochemistry of the two redox couples,

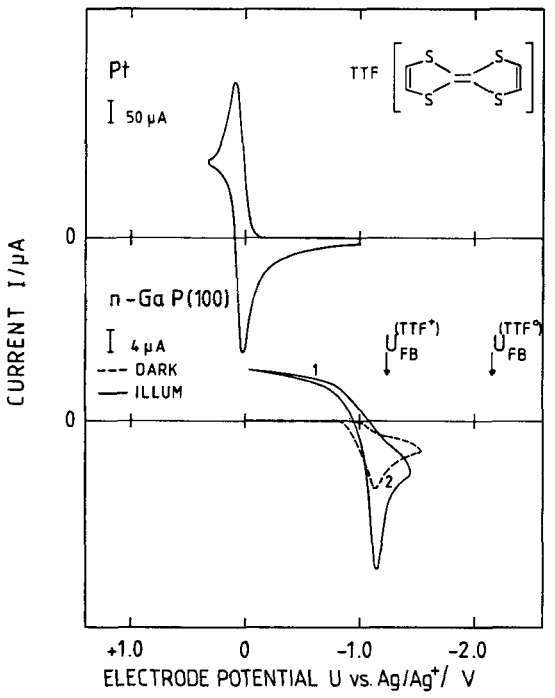

Fig. 7
Current-potential curves for ACN/TMABF (0.5 M), TTF (0.05 M), sweep rate 0.05 V s^{-1}: for Pt (A ~ 1.0 cm^2); for n-GaP (100) (A = 0.06), 1. Illum. ×0.2 attenuation, 2. Dark current in the presence of $TTF^{+\cdot}$ (~ 0.06 mM)

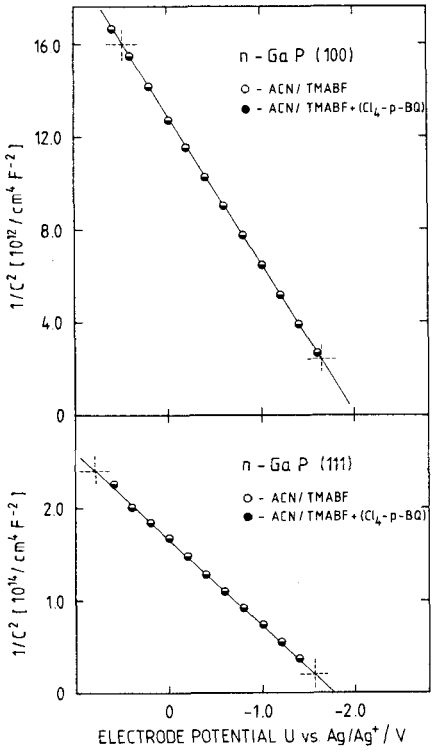

Fig. 8
Mott-Schottky plots for n-GaP (100) and n-GaP (111) in the absence of O-TCBQ, ○ – 1 kHz, and in the presence of O-TCBQ, ● – 1 kHz

o-TCBQ/o-$TCBQ^{-\cdot}$ and $TTF^{+\cdot}/TTF^0$, at n-GaP represents an ideal opportunity to distinguish between intrinsic surface states and surface states resulting from adsorption. Fig. 8 shows a comparison of the Mott-Schottky plots in the presence and absence of o-TCBQ at both n-GaP (100) and n-GaP (111) surfaces, U_{FB} is shown to be independent of the presence of o-TCBQ. Fig. 9 shows the current potential curves for the electroreduction of o-TCBQ occurring at the Pt-electrode, the process is shown to occur by two successive one electron transfer steps to produce the radical anion (U^0 ~ 0.0 V) and the dianion (U^0 ~ 0.9 V), respectively. The photo/dark-current curves are also presented for the same process occurring at n-GaP (100) and (111) surfaces. Although the light intensity incident on the electrode is somewhat reduced, due to absorption of the solution in the energy range corresponding to the band gap, the results are otherwise fully consistent with theoretical predictions.

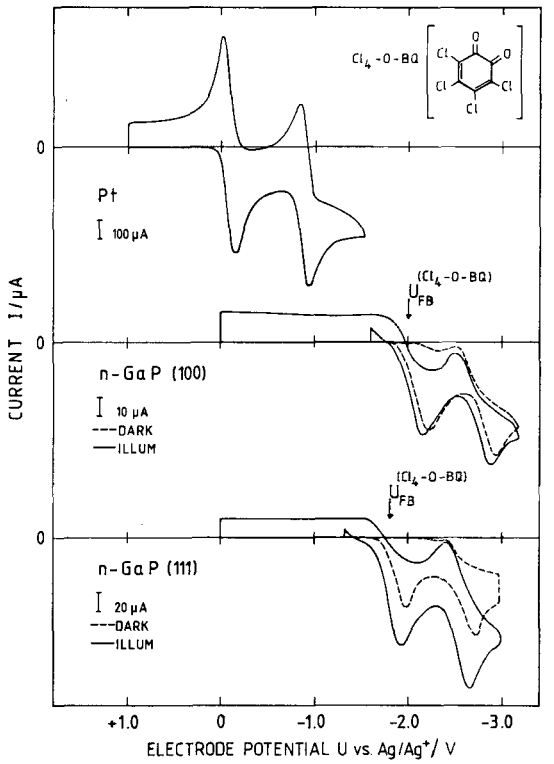

Fig. 9
Current-potential curves for ACN/TMABF (0.5 M), O-TCBQ (0.085 M), sweep rate 0.05 V s^{-1}: for Pt (A = 1.0 cm^2); for n-GaP (100) (A = 0.06 cm^2), 1. Illum. ×1 attenuation, 2. Dark current in the presence of O-TCBQ (0.085 M); for n-GaP (111) (A = 0.09 cm^2), 1. Illum. ×1 attenuation, 2. Dark current in the presence of O-TCBQ (0.085 M)

3.5. Capacitance Measurements After Illumination

According to the energy diagram described in Fig. 1 A, illumination of the electrode with sub-bandgap energy $E > E_{CB}^s - E_D^s$, for values of $E_F < E_D^s$, should ionize the proposed surface states, which once again would manifest itself as a positive shift in U_{FB}. This is shown schematically in Fig. 10. Fig. 11 A shows the normal Mott-Schottky plot obtained for n-GaP (100) in ACN/0.5 M TMABF. Fig. 11 B shows the Mott-Schottky plot obtained from the differental capacitance curve recorded, in a positive direction from + 0.4 V to – 1.6 V, after illumination at + 0.4 V with monochromatic light, λ = 900 nm ≡ 1.4 eV. We see that the donor density (N_d) is increased for the positive sweep $N_b = 5 \cdot 10^{18}$ cm^{-3}, compared with a value of $N_d = 2.4 \cdot 10^{18}$ cm^{-3} for the reverse sweep. The expected increase can be explained by the ionization of deep lying bulk donor states, which normally exist as impurity atoms. With increasing negative potential these states are reoccupied, as predicted by Fermi statistics, and therefore on returning in a positive direction from U_{FB} the Mott-Schottky plot closely resembles that obtained normally, cf. Fig. 11 A. Furthermore, under no circumstances, i.e. for a longer period of illumination or with λ < 900 nm, could the observed results be interpreted by the ionization of a large concentration of surface states.

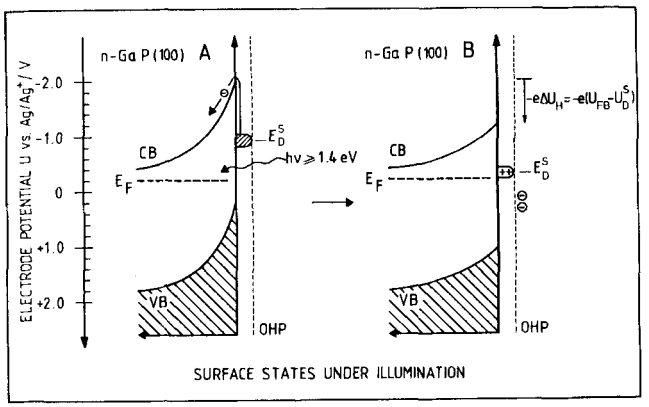

Fig. 10
Schematic representation of an electrode with a high density of donor surface states, located at a discrete energy (E_D^s) < 1.4 eV below the conduction band edge (E_{CB}^s), before and after illumination with $h\nu \geq 1.4$ eV, for the situation where the Fermi level is below the energy of the surface states

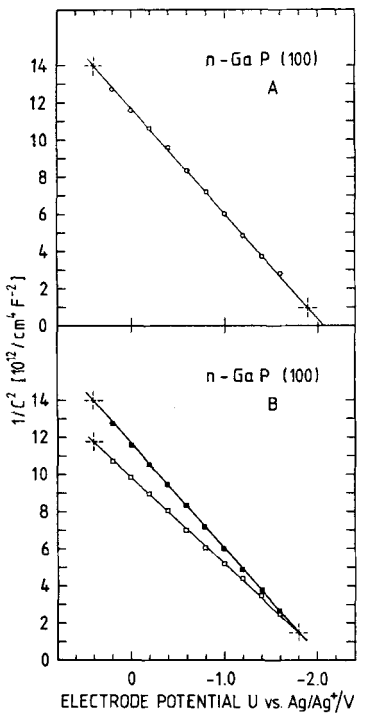

Fig. 11
Mott-Schottky plot for n-GaP (100) in ACN/TMABF (0.5 M); A – normal, B – after illumination for 2 mins with λ = 900 nm for the forward sweep (□) and for the reverse sweep (■)

4. Discussion

Considerable evidence has been presented to show that a positive shift in U_{FB} takes place in the presence of highly oxidising cations. However, as outlined in the introduction, the major problem is to identify the cause. The possibility of inversion, case 3 (sect. 1), can be excluded on two accounts. First, the redox couples are not sufficiently oxidising to cause such a large shift in U_{FB}. Second, under forward bias, the gradual release of positive surface charge to the bulk would result in a non-linear Mott-Schottky plot, this was not the case.

First consider the situation where intrinsic surface states are responsible for the observed shifts in U_{FB} as shown in Figs. 1A and 10. The requirement, therefore, would be a distribution of donor states, centering around an energy E_D^s (i.e. such that there is no net surface charge when the states are occupied to an energy level E_D^s). The occupation by electrons is controlled by Fermi statistics, thus the number of neutral donor states is given by [11 – 13]

$$N_{D(s)}^0 = N_{D(s)}\,[1 + g_D^s \exp[(E_D^s - E_F) - e_0(\phi_B - \phi_S)]/kT]^{-1} \quad (1)$$

where g_D^s is the degeneracy of the donor states and $N_{D(s)}$ is the total concentration of surface donors.

If we now assume a value of $(\phi_B - \phi_S)$ such that the states are completely full, we can write the equation for the surface donor charge as

$$q_D^s = e_o\, N_{D(s)}\,. \quad (2)$$

Given that the Helmholtz capacitance for a degenerate semiconductor is of the order of 10 μC cm^{-2} [14] then from Eq. (3)

$$\Delta\phi_H = \frac{q_o^s}{C_H} \quad (3)$$

for a potential drop in the Helmholtz layer $\Delta\phi_H$ = 1.0 V the surface charge $q_o^s = 10^{-5}$ C cm^{-2}. Substituting this value into Eq. (2) gives a value $N_{D(s)} \sim 10^{14}$ cm^{-2}, which is of the order of 10% of the surface atoms.

Two attempts were made to try and identify a large concentration of donor surface states at both n-GaP (100) and n-GaP (111) surfaces. First, for a large concentration of donor surface states, centered around 1.2 eV positive of E_{CB}^s, it should have been possible to ionize these states by illumination, with $h\nu \geq 1.2$ eV, the results presented in sec. 3.5 show that the effect of illuminating the electrode with λ = 900 nm = 1.4 eV was merely to ionize a small amount of neutral bulk donor states. Second, consider the very different behaviour of the two redox couples TTF, sec. 3.3, and o-TCBQ, sec. 3.4. Despite very similar redox potentials the presence of the $TTF^{+\cdot}$ ion was shown to cause a considerable positive shift in the value of U_{FB} Fig. 12B. This phenomenon was not observed under similar conditions in the presence of o-TCBQ, see Fig. 12A. Further-

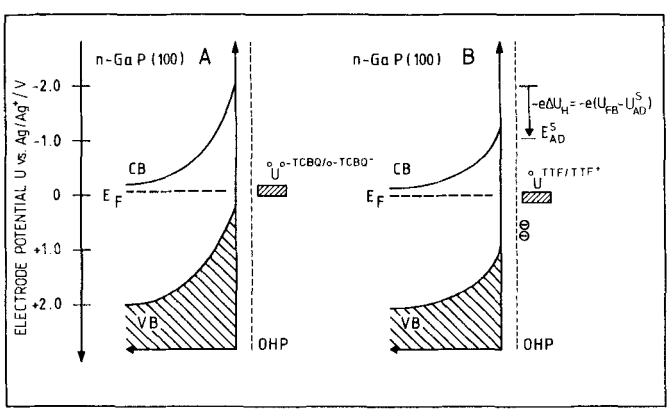

Fig. 12
Schematic representation of the Energy diagrams for n-GaP (100) with respect to the redox couples; Tetrachloro-o-benzoquinone (O-TCBQ) and tetrathiafulvalen (TTF). The potential scale is with respect to the Ag/Ag^+ (10^{-4} M) ref. electrode in ACN

more, electroreduction of the respective species is shown to occur at potentials which correspond well with the values of U_{FB} in the presence of the oxidised species. The inference, therefore, is that the difference in behaviour is due to the adsorption of the radical cation.

5. Conclusions

On the basis of the above results and discussion the reduction of strongly oxidising cations at n-GaP surfaces in ACN can be explained by direct electron transfer from the conduction band via the adsorbed cationic species, see Fig. 1B. The model which proposes mediated electron transfer via "deep-lying" surface traps which "pin" the Fermi-level of the semiconductor at or near the value of E_{trap} rather than E_{FB} [1] cannot be substantiated, in the case of n-GaP, based on the above results. The results of Kohl and Bard which seem to support the phenomenon of Fermi level pinning can be explained by the strong adsorption of the cationic component of the 10-MP/10-MP$^{+\cdot}$ redox couple, which results in a considerable positive shift in the band edges.

The authors are indebted to Dr. W. Storck for preparation and purification of 10-methylphenothiazine and for his helpful guidance concerning the purification of other compounds. One of us, R. M., would like to thank the Max-Planck-Gesellschaft for support during this period of study.

References

[1] P. A. Kohl and A. J. Bard, J. Am. Chem. Soc. *99*, 7531 (1977).
[2] H. Gerischer, Advances in Electrochemical Engineering, Vol. 1, Ed. P. Delahay, Interscience Publ., p. 139 and references therein, New York, London 1961.
[3] O. R. Brown and R. McIntyre, Electrochim. Acta *29*, 997 (1984).
[4] W. H. Chang, J. Org. Chem. *27*, 2921 (1962).
[5] D. O. Cowan et al., J. Org. Chem. *40*, 3544 (1975).
[6] S. Miller, J. A. Tebboth, and J. F. Tremaine, J. Chem. Soc. 632 (1952).
[7] J. P. Billon, Ann. Chem. *7*, 196 (1962).
[8] W. Ranke, Phys. Rev. *B27*, 7807 (1983).
[9] R. L. Meek and N. E. Schumaker, J. Electrochem. Soc. *119*, 1148 (1972).
[10] R. McIntyre, B. Smandek, and H. Gerischer, in preparation.
[11] M. Green, in: "Modern Aspects of Electrochemistry", Vol. 2, p. 356–381, Ed. J. O'M. Bockris, Butterworths, London 1959.
[12] M. Green, J. Chem. Phys. *31*, 200 (1959).
[13] H. Gerischer, in: "Physical Chemistry – An Advanced Treatise", Vol. IX A, p. 467–497, Eds. H. Eyring, D. Henderson, and W. Jost, Academic Press, New York 1970.
[14] R. McIntyre and H. Gerischer, to be published.

(Eingegangen am 22. Mai 1984, endgültige Fassung am 5. Juli 1984) E 5730

Photo-Chemistry of Colloidal Metal Sulfides 8. Photo-Physics of Extremely Small CdS Particles: Q-State CdS and Magic Agglomeration Numbers

A. Fojtik, H. Weller, U. Koch, and A. Henglein

Hahn-Meitner-Institut für Kernforschung Berlin, Bereich Strahlenchemie, D-1000 Berlin 39, Federal Republic of Germany

Catalysis / Colloides / Fluorescence / Photochemistry / Semiconductors

Extremely small CdS particles were prepared in propanol-2 solution at −78°C and in aqueous solution in the presence of sodium hexametaphosphate at room temperature. These colloids are colorless. Their UV absorption spectra exhibit several maxima. Aging of the colloids is accompanied by intensity variations in the absorption maxima and by a shift of the onset of absorption to longer wavelengths. These small CdS particles hardly possess semiconductor properties (Q-state CdS). A semi-classical treatment of the energies of an electron-hole pair in these particles yielded the wavelengths of their absorption spectra. At the small particle sizes used, the first excited state was reached by photon-absorption in the UV, and the second excited state was generally not reached at all. The various maxima in the absorption spectra are explained in terms of a size distribution of the colloids with preferential agglomeration numbers. Reasons for the formation of such a structured size distribution are given. The fluorescence and fluorescence excitation spectra of the small particles were also investigated. Particles below a certain size have only one broad fluorescence band at a much longer wavelengths than the onset of absorption. As the particle size increases, this band is shifted towards longer wavelengths, and finally an additional rather sharp band appears at the threshold of absorption. CdS colloids in the Q-state can be made which fluoresce as desired anywhere between the red and the blue. Also reported are the first experiments in which the preparation of Q-type CdS in the solid state is achieved by evaporating the solvent from the colloidal solutions.

Introduction

In the previous papers of this series, CdS and ZnS were found to fluoresce in the colloidal state, and it was further observed that these fluorescences could be quenched by solutes at low concentration, and that these colloids can act as catalysts for various photochemical reactions. In the last paper attention was drawn to the photo-physics of extremely small ZnS particles and it was pointed out that the particles lose their semiconductor properties as they become smaller and smaller [1]. Brus and coworkers [2–4] have made similar observations on CdS, where significant changes in the optical absorption spectrum occurred at particle sizes below 5 nm.

In the present paper, various methods are reported for the preparation of extremely small and fairly stable CdS particles in solution and even in the solid state. The optical absorption spectra, the fluorescence spectra, and the fluorescence excitation spectra of these colloids are reported. A difficulty in the preparation of colloidal CdS by precipitation of Cd^{2+} by added H_2S consists of the fact that a certain size distribution will always be produced instead of a monodisperse system. A sur-